

Magnetic Resonance Imaging Features of a Juxtaglomerular Cell Tumor

Suhai Kang, Aitao Guo¹, Haiyi Wang, Lu Ma, Zongyu Xie², Jinglong Li³, Xinyuan Tonge⁴, Huiyi Ye

Department of Radiology, ¹Department of Pathology, ⁴Statistical Teaching and Research Section, Chinese PLA General Hospital, Beijing, ²Department of Radiology, First Affiliated Hospital of Bengbu Medical College, Anhui Province, ³Department of MRI, First Hospital of Qinhuangdao, Hebei Province, PR China

Address for correspondence:

Dr. Huiyi Ye,
 Department of Radiology, Chinese PLA
 General Hospital, Beijing 100853,
 PR China.
 E-mail: 13701100368@163.com



Received : 19-11-2015

Accepted : 24-12-2015

Published : 31-12-2015

ABSTRACT

Objective: To retrospectively determine whether magnetic resonance imaging (MRI) findings can help differentiate a juxtaglomerular cell tumor (JCT) from clear cell renal cell carcinoma (ccRCC). **Materials and Methods:** Eight patients with JCTs and 24 patients with pathologically proven ccRCC were included for image analysis. All patients underwent unenhanced MRI and dynamic contrast-enhanced MRI. Fat-suppressed T2-weighted imaging (T2WI), diffusion-weighted imaging (DWI), in- and opposed-phase imaging, and fat-suppressed pre-contrast acquisitions with volume acceleration sequences were performed before enhancement. After the administration of contrast, dynamic imaging was performed in the corticomedullary, nephrographic, and excretory phases. Student's *t*-test, *t'*-test, Chi-square test, and nonparametric Kruskal–Wallis *H*-test were used to determine the significance of the difference between the two groups. The sensitivity and specificity of the MRI findings were calculated. **Results:** In patients with a JCT, a cystic part of the lesion of <10%, isointensity or mild hyperintensity on T2WI, heterogeneous hyperintensity on DWI, less signal drop (<10%) in in- and opposed-phase imaging, and a degree of enhancement <200% in the corticomedullary phase showed statistically significant differences compared with those of ccRCC ($P < 0.05$). After combining a lower apparent diffusion coefficient (ADC) value (heterogeneous hyperintensity) on DWI and a degree of enhancement <200% in the corticomedullary phase using a parallel test, the sensitivity and specificity were 90.9% and 91.7%, respectively. **Conclusions:** Isointensity or mild hyperintensity on T2WI, a lower ADC value (heterogeneous hyperintensity) on DWI, and a degree of enhancement <200% in the corticomedullary phase are the major MRI findings for JCTs, combined with relative clinical manifestations and excluding other renal masses. A main solid tumor, less signal drop (<10%) in in- and opposed-phase imaging, and a less-washout pattern of <10% in the delayed phase are secondary MRI findings for JCTs.

Key words: Clear cell renal cell carcinoma, combination, juxtaglomerular cell tumor, magnetic resonance imaging findings

Access this article online

Quick Response Code:



Website:

www.clinicalimagingscience.org

DOI:

10.4103/2156-7514.172976

This is an open access article distributed under the terms of the Creative Commons Attribution-NonCommercial-ShareAlike 3.0 License, which allows others to remix, tweak, and build upon the work non-commercially, as long as the author is credited and the new creations are licensed under the identical terms.

For reprints contact: reprints@medknow.com

How to cite this article: Kang S, Guo A, Wang H, Ma L, Xie Z, Li J, Tonge X, Ye H. Magnetic Resonance Imaging Features of a Juxtaglomerular Cell Tumor. J Clin Imaging Sci 2015;5:68. Available FREE in open access from: <http://www.clinicalimagingscience.org/text.asp?2015/5/1/68/172976>

INTRODUCTION

A juxtaglomerular cell tumor (JCT) of the kidney, also called reninoma, is a rare renal neoplasm first described by Robertson et al., in 1967.^[1] A JCT may cause hypertension and hypokalemia and generally occurs in adolescents and young adults.^[2] It may result in a cerebrovascular accident and even death.^[3-5] For this reason, early diagnosis and selective management are essential for adolescents and young adults. Although the clinical features of a JCT have been described in a few studies,^[6-8] it can be difficult to distinguish from other renal tumors because its clinical presentation and imaging findings are similar to those of renal cell carcinoma (RCC).^[6,9]

The standard surgical technique of nephron-sparing surgery for RCC involves excising an additional 1 cm margin of peritumor renal parenchyma to ensure a true negative margin and decrease the risk of local recurrence.^[10] A benign renal tumor could avoid the excision of additional peritumor renal parenchyma. As a rare renal tumor, a JCT is often regarded as a malignant tumor in terms of treatment. Therefore, it is essential to differentially diagnose malignant and benign renal tumors in young patient with renal masses.

Our retrospective study of 8 cases is, to the best of our knowledge, the largest study reported in the literature about JCTs. The purpose of our study was to document the magnetic resonance imaging (MRI) findings of JCTs and to analyze whether MRI characteristics can help distinguish a JCT from ccRCC and become the basis of effective therapy.

MATERIALS AND METHODS

The procedures of this study were in accordance with the ethical standards of the World Medical Association (declaration of Helsinki). Our Institutional Review Board approved this retrospective study. All patients agreed to the use of their imaging studies for medical analysis.

Study design

A retrospective review of the pathology database from January 2010 to March 2015 was performed for patients who underwent surgery for a renal neoplasm at our institution. The study was conducted with two sets of patients. The first group included eight cases of JCT. The second was the control group, which included 24 cases of ccRCC randomized from 69 ccRCC patients with size-matched tumors <5 cm.^[11] As ccRCC accounts for 70–80% of RCC cases,^[12] it first needs to be distinguished from a JCT.

The 69 cases selected from 295 patients were randomized by patients' serial number according to when each procedure was performed. Using SPSS v. 17.0 software (IBM Corp., Armonk, NY, USA), 24 randomized numbers were generated to populate the control group. Of the 8 JCT cases, 7 were grade 3 hypertension, 2 had slight hypokalemia (3.01–3.5 mmol/l), and 3 had moderate hypokalemia (2.5–3.0 mmol/l). The other clinical information for the two groups is shown in Table 1.

All patients in this cohort study met certain inclusion criteria. First, all patients had undergone unenhanced and enhanced MRIs, and images had to be available in a standard digital imaging format. Second, the MRIs had to be performed on patients without adrenal diseases or renal artery stenoses. Third, the size of the ccRCC mass had to be <5 cm because the mean size of the JCTs was 4.6 cm.^[11] Within this cohort of patients, 226 were excluded for the following reasons. First, patients were excluded if they had cystic ccRCC or a mass >5 cm, if the solid component of the lesion was too small to measure, or if they had another type of RCC. Second, patients were excluded if they had renovascular disease (renal artery stenosis), renal parenchymal disease (renal dysplasia, scarring, glomerulonephritis), or other renin-secreting tumors (e.g. Wilms' tumor).

Magnetic resonance imaging technique

MRI examinations were performed with 1.5- and 3.0-T systems (TwinSpeed Signa Excite HD, GE Healthcare, Milwaukee, WI, USA). For the morphologic evaluation of the renal tumors, respiratory-triggered transverse and coronal T2-weighted (T2W) fast spin-echo sequences were initially performed, followed by transverse T1W dual-echo in- and opposed-phase sequences. Diffusion-weighted imaging (DWI) was performed before the dynamic contrast-enhanced (DCE)-MRI with b values of 0 and 800 s/mm², and three-dimensional (3D) fat-saturated T1W DCE sequences were performed during suspended respiration. For the 3D DCE sequences, the section thickness was 5 mm and the interpolated section thickness was 1–1.5 mm. Gadopentetate dimeglumine (Consun, Guangzhou, China) was injected intravenously as a rapid bolus of 0.1–0.15 ml/kg at a rate of 2 ml/s with a power

Table 1: The clinical information of a juxtaglomerular cell tumor and clear cell renal cell carcinoma

Qualitative variable	Case group	
	JCT (n=8)	ccRCC (n=24)
Gender (female/male)	4/4	7/17
The range of age (year)	14-30	29-80
Size (cm, mean ± SD)	3.025 ± 0.734	3.354 ± 0.982

SD: Standard deviation, JCT: Juxtaglomerular cell tumor, ccRCC: Clear cell renal cell carcinoma

injector (Spectris; Medrad, Warrendale, PA, USA), followed by a 20-ml saline flush. DCE-MRI was performed in the transverse plane at baseline (precontrast) and during the corticomedullary, nephrographic, and excretory phases. The scan delays were 20–22 s for the corticomedullary phase, 100–120 s for the nephrographic phase, and 240 s for the excretory phase.

Several MRI findings for JCTs and ccRCC were analyzed, including location; pseudocapsule; T2W image (T2WI); T1WI; DWI; solid and cystic parts of the tumor (the cystic part included necrosis and hemorrhage); signal intensity (SI) of in- and opposed-phase images; corticomedullary, nephrographic, and excretory phases; and enhancement pattern.

Qualitative magnetic resonance image analysis

Before administration of the contrast agent, the location of tumor, the pseudocapsule, and the signals on T2WI and T1WI were analyzed independently by three radiologists (when the results differed between the first two, the third radiologist made a final decision) to assess the characteristics of the renal mass. The location of the tumor was indicated as pelvis parenchyma, intra-parenchyma, or intra- and outer-parenchyma. The pseudocapsule was shown by the entire or partial lower ring rather than by the cortex around the lesion on T2WI. On T2WI and T1WI, the signal of the tumor was divided into four or three groups: Lower intensity, iso or mild intensity, higher intensity than the SI of the renal parenchyma, and the heterogeneous signal. Necrosis and cystic degeneration showed a high SI on T2WI (although not as high as the SI of cerebrospinal fluid) and a low SI on T1WI and lacked enhancement. Hemorrhage, represented by nonenhanced areas, and sequelae of hemorrhage showed a high SI on T2WI that could not be suppressed on fat-saturated sequences [Table 2].

Quantitative magnetic resonance image analysis

All data in this study were stored in a picture archive and communication system (PACS). The signal index in the renal lesions was measured by one radiologist. The apparent diffusion coefficient (ADC) value of every tumor was measured on DWI using a commercially available software workstation system (Advantage Workstation, version 4.2; GE Healthcare, Bue, France) [Table 3].

A region-of-interest (ROI) was placed in the center of the most enhanced solid part of the tumor and encompassed at least two-thirds of its solid component. The area, location, and size of the ROI were the same in the in- and opposed-phase images; the precontrast liver acquisitions with volume acceleration (LAVA); and the corticomedullary,

Table 2: Univariate analysis of qualitative magnetic resonance imaging findings of a juxtaglomerular cell tumor and clear cell renal cell carcinoma

Qualitative variable	Case group			
	JCT (n=8)		ccRCC (n=24)	
	Reader 1	Reader 2	Reader 1	Reader 2
Location				
Parenchyma and pelvis	1	1	5	5
Intra-parenchyma	6	6	6	6
Intra- and out-parenchyma	1	1	13	13
T2WI SI				
Lower	1	1	0	0
Isointensity or mild higher	7	7	1	1
Higher	0	0	4	4
Heterogeneous	0	0	19	19
T1WI SI				
Lower	1	1	3	3
Isointensity or mild hypointensity	6	6	19	19
Higher	1	1	2	2
Pseudocapsule				
Positive	7	7	16	17
Negative	1	1	8	7

ccRCC: Clear cell renal cell carcinoma, DWI: Diffusion-weighted imaging, JCT: Juxtaglomerular cell tumor, SI: Signal intensity, WI: Weighted imaging

Table 3: Univariate analysis of quantitative magnetic resonance imaging findings of a juxtaglomerular cell tumor and clear cell renal cell carcinoma

Quantitative variable	Case group	
	JCT (n=8)	ccRCC (n=24)
Cystic degeneration and necrosis (%)		
Slight (< 10 section)	5	5
Slight moderate (11-30 section)	2	1
Moderate (31-50 section)	1	2
Severe (> 51 section)	0	16
In- and opposed-phase - SI decreased (%)		
< 10	7	11
11-20	1	5
21-30	0	3
> 31	0	5
Corticomedullary phase - SI increased (%)		
0-100	5	2
101-200	2	7
201-300	1	11
> 301	0	4
Nephrographic phase - SI increased (%)		
0-100	2	1
101-200	2	6
201-300	4	12
> 301	0	5
Excretory phase - SI increased (%)		
0-100	2	4
101-200	2	8
201-300	4	10
> 301	0	2

ccRCC: Clear cell renal cell carcinoma, JCT: Juxtaglomerular cell tumor, SI: Signal intensity

nephrographic, and excretory phases. Care was taken to skirt the edge of the tumor near the interface with the adjacent perirenal fat to avoid a phase cancellation artifact.

Mean SI measurements were recorded in arbitrary units. The SI indexes were calculated as $(\text{tumor SI}_{\text{in}} - \text{tumor SI}_{\text{opp}}) / \text{SI}_{\text{in}}$, where SI_{in} represents the SI on the in-phase images and

SI_{opp} represents the SI on the opposed-phase images; as $(\text{tumor } SI_{cor} - \text{tumor } SI_{pre})/SI_{pre}$, where SI_{cor} represents the SI on the corticomedullary phase images and SI_{pre} represents the SI on the precontrast LAVA images; as $(\text{tumor } SI_{neph} - \text{tumor } SI_{pre})/SI_{pre}$, where SI_{neph} represents the SI on the nephrographic phase images; and as $(\text{tumor } SI_{exc} - \text{tumor } SI_{pre})/SI_{pre}$, where SI_{exc} represents the SI on the excretory phase images.

To measure the scope of cystic degeneration or necrosis, a tool-measuring area in the PACS was used to delineate the shape of the entire tumor and its cystic component. First, in the cross-section imaging of maximum diameter on T2WI, the profile of the whole lesion was curved along the margin of the lesion or the cystic degeneration or necrosis component. The ratio was then calculated as $\text{tumor } S_{cys} : \text{Tumor } S_{ent}$, where S_{cys} represents the area of the cystic proportion of the tumor and S_{ent} represents the area of the entire tumor [Table 2].

Pathologic analysis

To confirm the diagnosis of either a JCT or ccRCC in all patients, pathologic specimens were reviewed retrospectively by a pathologist according to the World Health Organization 2004 pathologic diagnostic criteria.^[13] Immunohistochemical studies were performed, and the cytoplasm of the tumor cells expressed renin. Abundant endoplasmic rhomboid crystalline renin granules were found ultrastructurally.

Statistical analysis

For the normal distribution data, Student's *t*-test was used. For the nonnormal distribution data, the *t'*-test was used. To analyze the relationships among the quantitative data, they were transformed into grade data. The nonparametric Kruskal–Wallis *H*-test or the Chi-square test was used to compare the differences between the two groups.

For qualitative data, κ values were calculated to assess interreader agreement for the following qualitative variables: 0 = no agreement; 0.01–0.20 = slight agreement; 0.21–0.40 = fair agreement; 0.41–0.60 = moderate agreement; 0.61–0.80 = substantial agreement; 0.81–1.0 = almost perfect agreement. If the qualitative data fit for the normal distribution, the Chi-square test was used. All analyses were performed with SPSS v. 19.0 software (IBM Corp, Armonk, NY, USA) and CHISS software (<http://www.chiss.cn>). $P < 0.05$ was considered significant. The sensitivity, specificity, accuracy rate, and Youden's index of MRI findings were calculated. The highest sensitivity or specificity of the MRI finding was chosen to conduct parallel and series tests.

RESULTS

Location, T2- and T1-weighted images, solid and cystic proportions of a juxtaglomerular cell tumor

The κ values were calculated with the findings of location, T2WI, T1WI, and the solid and cystic proportions. All κ values were 1.

Most tumors in patients with JCT (6/8) were located in the intra-parenchyma, 1 tumor protruded to the pelvis, and 1 markedly protruded out to the parenchyma. The difference in the number of tumors in the intra-parenchyma and intra- and outer-parenchyma for JCTs and ccRCC was statistically significant ($P < 0.05$).

Most patients with JCTs (5/8) showed solid tumors [Figure 1a and b]. Solid JCTs showed isointensity or mild hyperintensity on T2WI and isointensity or mild hypointensity on T1WI. Of the 8 patients with JCTs, 3 showed solid and cystic tumors [Figure 2a and b]. The differences between the group with isointensity or mild hyperintensity and hyperintensity and the group with isointensity or mild hyperintensity and heterogeneous hyperintensity for JCTs and ccRCC were statistically significant on T2WI ($P < 0.05$ and 0.01), but not statistically significant ($P > 0.05$) on T1WI.

Solid tumors were more frequent in JCTs than in ccRCC ($P = 0.0107$). In addition, the cystic part of the tumor being $< 10\%$ of the area was more likely in JCTs than in ccRCC ($P < 0.05$).

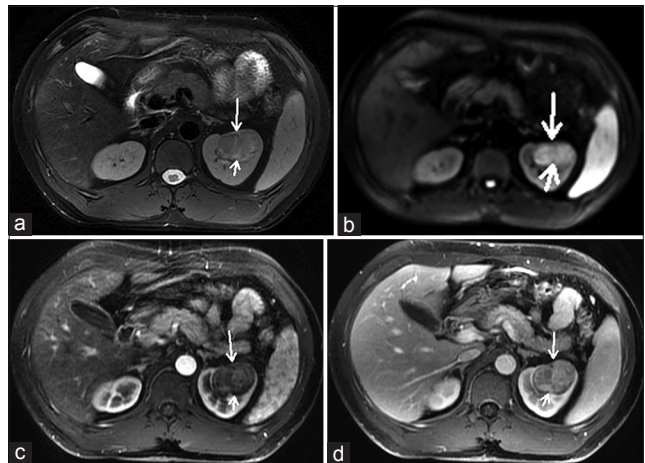


Figure 1: 28-year-old man with Grade 3 hypertension for 7 years with a solid tumor on the left kidney and the pathological diagnosis was juxtaglomerular cell tumor after surgery. (a) On T2-weighted image, the lesion (short arrow) shows isointensity to mild hyperintensity with a low-signal capsule (long arrow). (b) On diffusion-weighted image, the lesion (short arrow) indicates heterogeneous hyperintensity compared with the cortex signal and the low-signal capsule (long arrow) does not indicate clearly. (c) On the corticomedullary phase image, the lesion (short arrow) shows mild enhancement. (d) On the nephrographic phase image, the lesion (short arrow) shows a mild persistent enhancement.

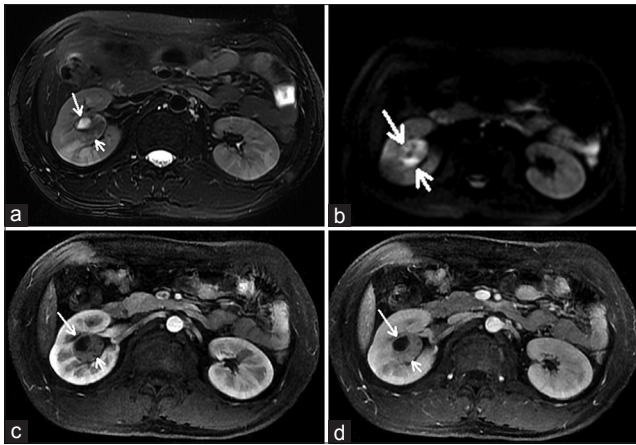


Figure 2: 23-year-old man with Grade 3 hypertension for 4 years with a solid and cystic tumor near the right renal pelvis and the pathological diagnosis was juxtaglomerular cell tumor after surgery. (a) On T2-weighted image, the lesion shows heterogeneous hyperintensity without a low-signal capsule, the solid part of the lesion (short arrow) shows heterogeneous hyperintensity, the cystic part of the lesion (long arrow) shows hyperintensity. (b) On diffusion-weighted image, the solid part of the lesion (short arrow) indicates heterogeneous hyperintensity, the cystic part of the lesion (long arrow) shows iso to mild hyperintensity. (c) On the corticomedullary phase image, the solid part of the lesion indicates a mild enhancement (short arrow). (d) On the nephrographic phase image, the solid part of the lesion (short arrow) shows a slight persistent enhancement.

Capsule or pseudocapsule

The capsule or pseudocapsule showed a slight circular hypointensity on T2WI [Figures 1a and 2a]. The κ values were calculated with these findings of the capsule or pseudocapsule. The κ value of the JCTs was 1 and the κ value of ccRCC was 0.9031. The difference between the sign of the pseudocapsule of ccRCC and the capsules of the JCTs was not statistically significant ($P = 0.7893$).

Diffusion-weighted images

The ADC value for the JCTs was lower than for ccRCC ($P < 0.0029$). The receiver operator characteristic (ROC) curve illustrated that the optimal cut-off value was 1.550 and Youden's index was 0.735. The area under the ROC curve (AUC) was 0.889 (95% CI: 0.000–1.000, Figure 3a).

In- and opposed-phase imaging

In in- and opposed-phase imaging, the signals of most JCTs (7/8) did not drop. As the amount of lipid in the tumor decreased, the probability of developing a JCT was higher than of developing ccRCC ($P = 0.0011$).

In accordance with the degree of signal drop, all cases could be divided into two groups of $<10\%$ and $>11\%$. Using the Chi-square test, the results showed that a patient with a lipid level of $<10\%$ in the tumor was more likely to develop a JCT than ccRCC ($P = 0.0094$).

Degree of enhancement in three phases

In the corticomedullary and nephrographic phases, the degree of enhancement of the JCTs was lower than that of

ccRCC ($P = 0.0010$ and $P = 0.0330$, respectively) [Figure 4]. The ROC curve illustrated that the optimal cut-off value was 1.270 (times) in the corticomedullary phase and Youden's index was 0.667. The AUC was 0.859 (95% CI: 0.674–1.000, Figure 3b).

Based on the degree of enhancement, all cases could be divided into two groups of $<200\%$ and $>200\%$. Five of the 8 cases of JCT showed a degree of enhancement $<100\%$ and only 1 enhancement was $>200\%$. The degree of enhancement in the corticomedullary phase of $<200\%$ showed a greater probability of developing a JCT than ccRCC ($P = 0.0269$). The map in Figure 4a and b indicates the enhanced mean value and enhanced trend between JCTs and ccRCC [Figures 1c, d and 2c, d].

Based on the drop in enhancement for tumors in the excretory phase, we classified the enhanced pattern into two types: A "less-washout" pattern of $<10\%$ (6/8:11/24) and a washout pattern of $>11\%$ (2/8:13/24). The less-washout pattern had a greater probability of developing a JCT than ccRCC in the excretory phase ($P = 0.0265$).

The validity of magnetic resonance imaging findings for differentiating a juxtaglomerular cell tumor and clear cell renal cell carcinoma

The validity of the isointensity or mild hyperintensity was highest on T2WI [Table 4]. After combining a lower ADC value on DWI and a degree of enhancement $<200\%$ in the corticomedullary phase using a parallel test, the sensitivity, specificity, accuracy rate, and Youden's index were 90.9%, 91.7%, 91.4%, and 0.826, respectively.

DISCUSSION

To date, approximately 110 cases of JCTs have been reported in the English literature.^[2,7,14-18] Studies with statistical evidence about MRI findings on JCTs are almost nonexistent beyond a few case reports.^[10,19]

Our statistical results indicate that JCTs are more likely to be located in the intra-parenchyma than in other areas. This may be related to the JCT originating from the modified smooth muscle cells that comprises the vascular component of the juxtaglomerular apparatus.^[20,21] Juxtaglomerular cells are near the pelvis parenchyma.

On T2WI, we classified JCTs into two types. One is the main solid component of the lesion. Most of our JCT cases (5/8) showed this characteristic, which we called typical JCT. It shows the characteristic finding of isointensity to mild hyperintensity on T2WI. The whole lesions in the remaining three patients in our study contained $<50\%$

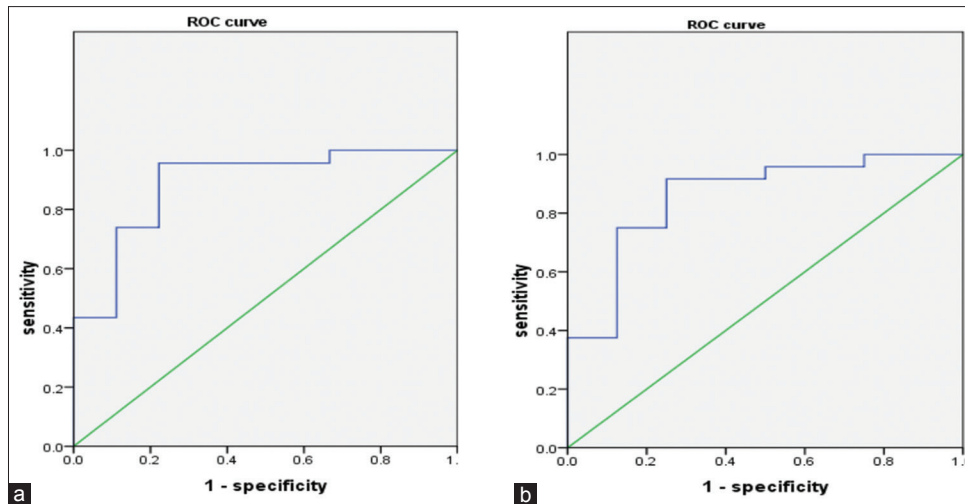


Figure 3: (a) The receiver operator characteristic curve of apparent diffusion coefficient. (b) Enhanced times in corticomedullary phase.

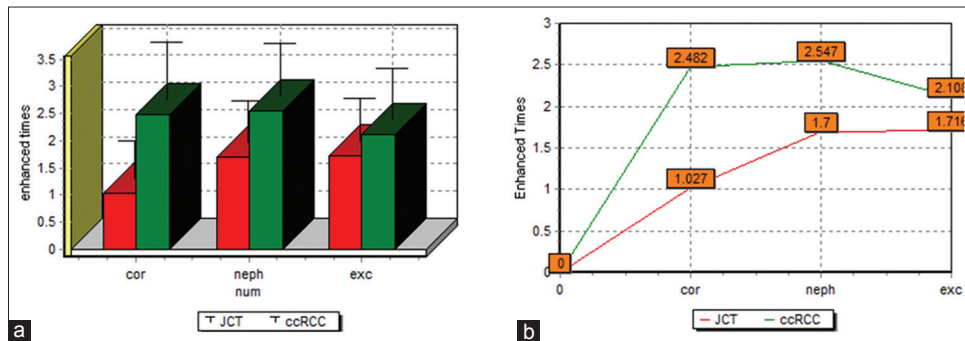


Figure 4: (a) The enhanced times in three phases between juxtaglomerular cell tumor and clear cell renal cell carcinoma. (b) The enhanced times of trend in three phases between juxtaglomerular cell tumor and clear cell renal cell carcinoma. Cor: Corticomedullary phase times, Neph: Nephrographic phase times, Exc: Excretory phase times.

Table 4: The validity of magnetic resonance imaging findings for differentiation between juxtaglomerular cell tumor and clear cell renal cell carcinoma

Index test	Validity			
	Sensitivity (%)	Specificity (%)	Youden's index	Accuracy rate (%)
Located in parenchyma or pelvis ①	87.5	54.2	0.417	62.5
Isointensity or mild hyperintensity on T2WI ②	87.5	95.8	0.833	93.8
Cystic degeneration and necrosis <0.1, ③	20.8	37.5	-0.417	25.0
Lower ADC value ④	91.7	91.7	0.834	87.5
In- and opposed-phase SI decreased <0.1, ⑤	87.5	54.2	0.417	62.5
Corticomedullary phase SI increased <1, ⑥	62.5	91.7	0.542	84.4
Excretory phase SI increased <0.1, ⑦	25.0	83.3	0.083	68.8
④ + ⑥ (parallel test)	90.9	91.7	0.826	91.4
④ + ⑥ (series test)	45.5	91.7	0.372	80.1

Parallel test: It means that the diagnostic result is positive when one of the diagnostic indexes is positive. The series test: It means that the diagnostic result is negative when one of the diagnostic indexes is negative, and the diagnostic result is positive when all of diagnostic indexes are positive. DWI: Diffusion-weighted imaging, SI: Signal intensity, WI: Weighted imaging, ADC: Apparent diffusion coefficient

cystic components, which we called atypical JCT. The solid components of the typical and atypical JCTs demonstrated similar SIs on T2WI. The SI of the cystic component indicated heterogeneous hyper- or hypo-intensity depending on the stage of hemorrhage. A JCT may have a less cystic component because the growth speed and the degree of vascularization in JCTs are lower than in ccRCC. Isointensity to mild hyperintensity on T2WI and the more solid

component of the tumor indicate a greater probability of a JCT.

As proven by pathology, a JCT is a well-circumscribed and complete or partial fibrous capsule that can be observed in most cases.^[20] A fibrous capsule and pseudocapsule always demonstrate a lower signal on T2WI. A pseudocapsule is a characteristic finding of RCC.^[22,23] Our statistical results

indicate that the complete or partial fibrous capsule of a JCT and the pseudocapsule of ccRCC are not distinguishable on T2WI. This is the most important contributor to the misdiagnosis of JCTs as RCC.

Our statistical results demonstrate that the ADC value of a JCT is lower than that of ccRCC. This means that the signal on DWI with a JCT is higher than with ccRCC and shows heterogeneous hyperintensity. The signal for DWI depends on tissue organization, cellularity, integrity of the cell membranes, extracellular space tortuosity, and increased cellular density.^[24] There are a few possible reasons why DWI shows a higher signal with a JCT than with ccRCC. The JCT tissue may have less internal necrosis, cystic degeneration, hemorrhage, and more cellular density than the ccRCC tissue because it is restricted to the molecular diffusion of water in the JCT tissues. Moreover, the cellularity and tissue organization might differ between JCTs and ccRCC.

Our statistical results indicate that the degree of signal drop for JCTs in in- and opposed-phase imaging is less than for ccRCC because JCTs lack an intermingling adipose tissue component.^[20] A smaller lipid component of the tumor indicates a greater probability of JCT compared with ccRCC.

The statistical results also indicate that most JCTs have less blood supply than ccRCCs. The renal angiographic findings also showed a hypovascular area or no abnormal vascularities.^[3,21,25] The pathology of the JCTs, however, contained a prominent vasculature.^[20] Our study and another report^[2] showed a mild enhancement in most cases of JCT. This might indicate that the contrast agent could not enter the vessel or diffuse easily into the tumor, possibly because most of the tumor vessel's function is abnormal (e.g. thick-walled vessels and hyalinosis).^[20] In the nephrographic phase, the degree of enhancement for JCTs was less than for ccRCC.

The statistical results demonstrate that no washout or a less-washout pattern of <10% in JCTs is a characteristic finding in the delayed phase in most cases. The drop in the degree of enhancement was <10% in 6 of 8 patients in our study. Two of the 8 cases exhibited the washout pattern, with a drop in the degree of enhancement of >11%. The reason for this might be that the contrast agent does not easily wash out from the neoplasm to the veins of the kidney.

Youden's indexes of isointensity or mild hyperintensity on T2WI and heterogeneous hyperintensity on DWI are higher than for other variables. The combination of a higher ADC value and a degree of enhancement <200% in the corticomedullary phase is one of the best diagnostic indexes for JCT.

Clinical presentation (age <30 years and Grade 2–3 hypertension) and laboratory examination (moderate hypokalemia) have important reference values for the diagnosis of JCT. This study was limited by the partly observational imaging findings. In addition, because of length restrictions, our paper did not distinguish other types of RCC.

CONCLUSION

In case of a renal mass, isointensity or mild hyperintensity on T2WI, a lower ADC value (heterogeneous hyperintensity) on DWI, and a degree of enhancement <200% in the corticomedullary phase are major MRI findings for JCT when combined with relevant clinical history and the exclusion of other renal masses. The main solid component of the tumor with less signal drop (<10%) in in- and opposed-phase imaging, and a less-washout pattern of <10% in the delayed phase are secondary MRI findings for JCT.

Acknowledgement

The authors would like to thank Dr. Xinyuan Tong and Dr. Xu Zhang for their contributions.

Financial support and sponsorship

Nil.

Conflicts of interest

There are no conflicts of interest.

REFERENCES

- Robertson PW, Klidjian A, Harding LK, Walters G, Lee MR, Robb-Smith AH. Hypertension due to a renin-secreting renal tumour. *Am J Med* 1967;43:963-76.
- McVicar M, Carman C, Chandra M, Abbi RJ, Teichberg S, Kahn E. Hypertension secondary to renin-secreting juxtaglomerular cell tumor: Case report and review of 38 cases. *Pediatr Nephrol* 1993;7:404-12.
- Brand G, Vandongen R, Beilin LJ, Matz L. Juxtaglomerular tumour: Diagnostic renal vein renin measurements obscured by chronic captopril therapy. *Aust N Z J Med* 1985;15:755-7.
- Gherardi GJ, Arya S, Hickler RB. Juxtaglomerular body tumor: A rare occult but curable cause of lethal hypertension. *Hum Pathol* 1974;5:236-40.
- Ørjavik OS, Fauchald P, Hovig T, Øystese B, Brodwall EK. Renin-secreting renal tumour with severe hypertension. Case report with tumour renin analysis, histopathological and ultrastructural studies. *Acta Med Scand* 1975;197:329-35.
- Osawa S, Hosokawa Y, Soda T, Yasuda T, Kaneto H, Kitamura T, et al. Juxtaglomerular cell tumor that was preoperatively diagnosed using selective renal venous sampling. *Intern Med* 2013;52:1937-42.
- Kuroda N, Gotoda H, Ohe C, Mikami S, Inoue K, Nagashima Y, et al. Review of juxtaglomerular cell tumor with focus on pathobiological aspect. *Diagn Pathol* 2011;6:80.
- Dong D, Li H, Yan W, Xu W. Juxtaglomerular cell tumor of the kidney – A new classification scheme. *Urol Oncol* 2010;28:34-8.
- Tanabe A, Naruse K, Kono A, Hase M, Hashimoto Y, Nakazawa H, et al. A very small juxtaglomerular cell tumor preoperatively identified by magnetic resonance imaging. *Intern Med* 1996;35:295-300.

10. Russo P. Renal cell carcinoma: Presentation, staging, and surgical treatment. *Semin Oncol* 2000;27:160-76.
11. Wong L, Hsu TH, Perlroth MG, Hofmann LV, Haynes CM, Katznelson L. Reninoma: Case report and literature review. *J Hypertens* 2008;26:368-73.
12. Reuter VE. The pathology of renal epithelial neoplasms. *Semin Oncol* 2006;33:534-43.
13. Eble JN, Sauter G, Epstein JI, Sesterhenn IA. World Health Organization Classification of Tumors. Pathology and Genetics of Tumors of the Urinary System and Male Genital Organs. 1st ed. Lyon: IARC Press; 2004. p. 72-3.
14. Kuroda N, Maris S, Monzon FA, Tan PH, Thomas A, Petersson FB, et al. Juxtaglomerular cell tumor: A morphological, immunohistochemical and genetic study of six cases. *Hum Pathol* 2013;44:47-54.
15. Shera AH, Baba AA, Bakshi IH, Lone IA. Recurrent malignant juxtaglomerular cell tumor: A rare cause of malignant hypertension in a child. *J Indian Assoc Pediatr Surg* 2011;16:152-4.
16. Ossareh S, Shooshtarizadeh T, Shadpour P. A 22-year-old woman with hypertension and hypokalemia due to a juxtaglomerular cell tumor. *Iran J Kidney Dis* 2011;5:425-8.
17. Jiang Y, Duan L, Lu L, Zhao WG, Zeng ZP, Li HZ, et al. Rare case of reninoma with double inferior vena cava. *Clin Exp Hypertens* 2011;33:325-7.
18. Lachvac L, Svajdler M, Valansky L, Nagy V, Benicky M, Frohlichova L, et al. Juxtaglomerular cell tumor, causing fetal demise. *Int Urol Nephrol* 2011;43:365-70.
19. Agrawal R, Jafri SZ, Gibson DP, Bis KG, Ali-Reza. Juxtaglomerular cell tumor: MR findings. *J Comput Assist Tomogr* 1995;19:140-2.
20. Martin SA, Mynderse LA, Lager DJ, Cheville JC. Juxtaglomerular cell tumor: A clinicopathologic study of four cases and review of the literature. *Am J Clin Pathol* 2001;116:854-63.
21. Hayami S, Sasagawa I, Suzuki H, Kubota Y, Nakada T, Endo Y. Juxtaglomerular cell tumor without hypertension. *Scand J Urol Nephrol* 1998;32:231-3.
22. Yamashita Y, Honda S, Nishiharu T, Urata J, Takahashi M. Detection of pseudocapsule of renal cell carcinoma with MR imaging and CT. *AJR Am J Roentgenol* 1996;166:1151-5.
23. Pretorius ES, Siegelman ES, Ramchandani P, Cangiano T, Banner MP. Renal neoplasms amenable to partial nephrectomy: MR imaging. *Radiology* 1999;212:28-34.
24. Subhawong TK, Jacobs MA, Fayad LM. Diffusion-weighted MR imaging for characterizing musculoskeletal lesions. *Radiographics* 2014;34:1163-77.
25. Moss AH, Peterson LJ, Scott CW, Winter K, Olin DB, Garber RL. Delayed diagnosis of juxtaglomerular cell tumor hypertension. *N C Med J* 1982;43:705-7.